The effects of contaminant ion species on thermonuclear ignition and burn in high density DT fuel

J. Pasley

University of York, Department of Physics, Heslington, York YO10 5DD, UK and Central Laser Facility, STFC, Rutherford Appleton Laboratory, HSIC, Didcot, Oxon OX11 0QX, UK

Contact | **jp557@york.ac.uk**

Introduction

In the re-entrant cone guided approach [1] to fast ignition [2] for inertial confinement fusion [3] the deuterium-tritium (DT) fuel in the imploding shell may become mixed with the material of the cone during flight. This can occur as a result of Kelvin-Helmholtz based mixing at the fuel/cone interface, Rayleigh-Taylor Instability induced mixing between the imploding shell and preheat ablated cone material, and mixing that occurs during the compression of the cone tip by the stagnating fuel core.

Mixing of high-Z material with the fuel inhibits the ignition and burn processes principally by enhancing the radiative cooling losses.

Problems arising from high-Z cone-fuel mix may potentially be tackled by tamping the cone with a lower-Z material [4], or employing a lower-Z material for the cone itself.

Methodology

In this study, a 1D Lagrangian radiation hydrodynamics simulation code, HYADES [5], employing multi-group diffusion for X-rays and charged particles is employed. Thermonuclear reactions may take place between the light isotopes. Only the most important reactions are considered. In addition, certain in-flight nuclear reactions (those between a thermal particle and an athermal particle) and elastic scattering reactions are performed.

Thermonuclear (Maxwell-averaged reactions:	Elastic scattering reactions:	In-flight reactions:
d(d,n)He-3	p,p	d(d,n)He-3
d(d,p)t	d,p	d(d,p)t
t(d,n)He-4	t,p	t(d,n)He-4
t(t,2n)He-4	He-3,p	He-3(d,p)He-4
He-3(n,p)t	He-4,p	d(t,n)He-4
He-3(d,p)He-4	d,d	d(He-3,p)He-4
He-3(t,d)He-4	t,d	
He-3(t,np)He-4	He-3,d	
He-3(He-3,2p)He-4	He-4,d	
	t,t	
	He-3,t	
	He-4,t	
	He-3,He-3	
	He-4,He-3	
	He-4,He-4	

The code can also incorporate a number of other reactions, not shown above, up to B-11. However these are switched off for the purposes of the current study.

Neutron reactions are not included in the present version of the code; neutrons can be either allowed to escape the problem or are deposited locally. Given the comparatively small scale of the target, neutrons are allowed to escape in the present study.

The multi-group diffusion model sets up energy bins for the reaction products. In the first case, for particle sym, there will be n1 'slow' groups and n2 'fast' groups. In the second case, the 'slow' groups will have group-centre energies from thermal to e1 (keV) and the 'fast' groups will have energies up to e2 (keV). The group assignments are shown in Table 1.

Sym	particle	n1	n2	e1	e2
n	neutron	5	8	2449	14060
p	proton	5	8	3023	14670
d	deuteron	5	8	2180	13050
t	triton	5	8	1011	12540
He-3	helium-3	5	8	820	12540
He-4	alpha	5	8	3542	12300

Table 1. Group assignments for the multi-group diffusion model employed for the reaction products.

In these runs we employ a high temperature (data to 172keV) SESAME equation of state file for DT.

Three different initial fuel configurations are employed for the ignition and burn problem. These are illustrated below in figure 1. In (I) the fuel starts off as a uniform sphere, which has been raised to some density, ρ, and heated to some temperature, T_{hot}. There is present in the fuel some concentration of impurities, n_{imp}, which is represented as a fraction of the total number of fuel ions. The second configuration (II) is similar to the first except that now the central hot region is surrounded by a cold region that is otherwise similar. In the third case, this surrounding region has no impurities present.

Further variety is added by considering a range of different contaminant ion species. Gold is considered, since this is the current 'default' cone material. Iron is considered, since it may have application in some

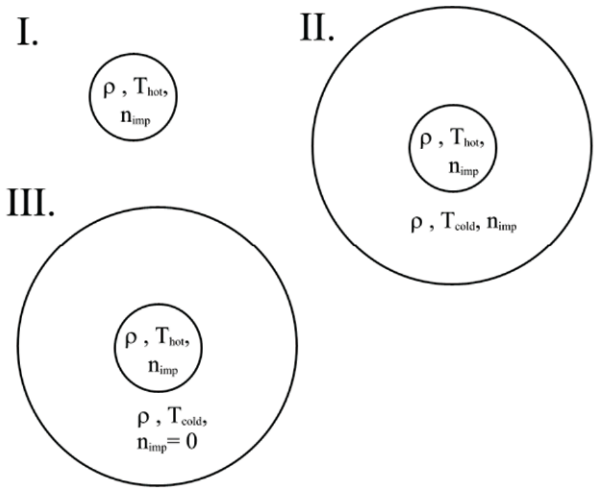

Figure 1. The three different fuel configurations employed in the simulations.

techniques for capsule injection (electromagnetic injection), finally CH is considered, since it is the most widely postulated cone tamping material.

Results

Type I.

The simulated object is a 200 μm radius sphere of fuel at a uniform density of 300 g/cm^3 raised to a uniform temperature of 5 keV.

In table 2, we compare the results of contamination by the three different contaminant ion species in terms of the final yield as a fraction of the yield from an uncontaminated target. Yield for the uncontaminated target is 17.4 MJ. Decompression halts the burn.

n_{imp}	C	Fe	Au
0.02	0.88	0.04	0.009
0.01	0.93	0.05	0.03
0.005	0.97	0.72	0.08
0.001	0.99	0.91	0.15
0.0002	0.99	0.98	0.8

Table 2. Yield (contaminated) / Yield (uncontaminated) for fuel configuration I.

Carbon is chosen as a contaminant material that is representative of a fuel tamping layer.

Figure 2 shows the motion of a gold surface tamped by a range of different materials, of differing thicknesses[4]. Peak displacement of the Au/tamper interface is shown from 1D radiation hydrodynamics simulations also performed using the HYADES code. Results are displayed for three cases representing cone ablation driven the X-ray radiation field anticipated in the interior of a capsule driven by both gold and uranium based hohlraums, as well as ablation driven by bremsstrahlung X-rays that have penetrated to the interior of a directly driven shell.

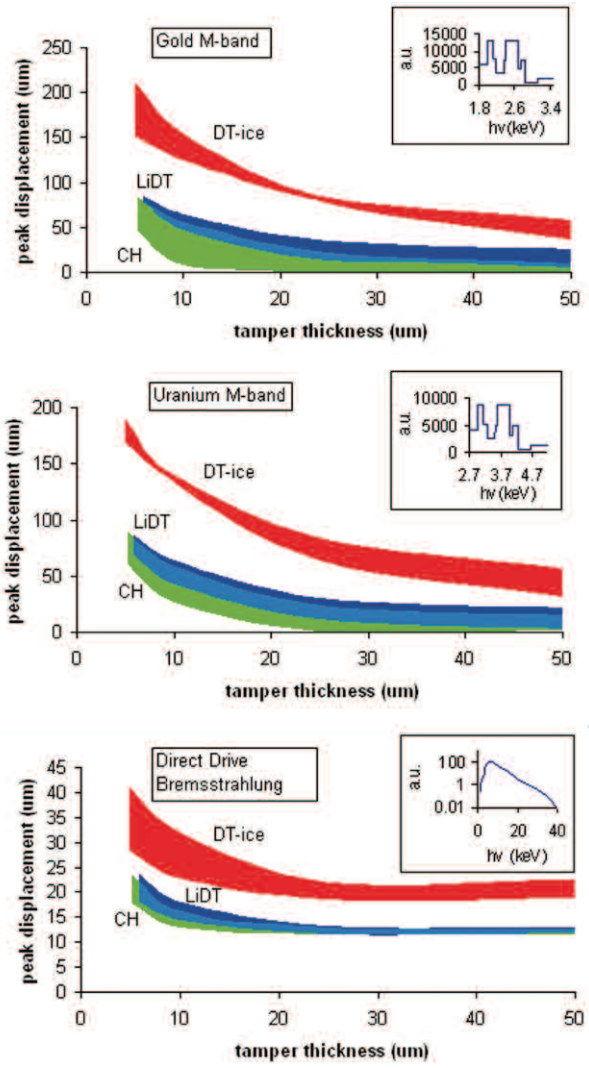

Figure 2. Effectiveness of various cone tamper materials.

Simulations were run to 2 ns in all cases. As can be seen from these results, carbon, in the form of solid density CH, is shown to be an excellent tamper material. In combination with the above data we can also see that the effect on thermonuclear burning is minimal.

Type II

As shown in figure 1, the central hot region is surrounded by a cold region of the same density and contamination fraction (Au contamination only is simulated), however at a much lower temperature, T_{cold}. In these simulations T_{cold} is set at a value of 50 eV. The radius of the hot central region is varied, whilst holding the outer radius of the cold fuel region constant. By iteration, the value of the critical burn-up parameter ($x_c = \rho r_{hot}$ for ignition) is found to the nearest 0.15 g/cm^2.

A range of different cold fuel outer radii have been explored extending from 200 μm to 5 mm. As expected, the outer radius of the cold fuel was found not to affect the success or failure of ignition, since the region is always of significantly greater thickness than the alpha deposition

range, and sufficiently thick to prevent decompression near the hot/cold boundary prior to ignition.

Table 3 shows the results of these simulations in terms of the critical burn-up parameter as a fraction of that in the uncontaminated case.

	n_{imp}	0	0.01	0.001
T_{hot}				
5keV		1	4.56	3.68
10keV		1	3.01	2.35

Table 3. Showing the ratio of critical burn-up parameters for Au contaminated fuel assemblies of type II.

Type III

In this case the central, contaminated, hot region is surrounded by cold fuel. However in this case the fuel is uncontaminated. Again T_{cold} = 50eV.

For type III fuel assemblies we compared the ignition with a 5 keV, 300 g/cm^3, 1% Au contamination against that from type II. Interestingly it was found that the normalised critical burn-up parameter increased relative to type II to a value of 5.02. This seems to be a consequence of the fact that the uncontaminated cold fuel does not trap the radiation from the hot region as effectively.

Conclusions

The results of the simulation study clearly show the detrimental effect of high-Z (Au) contamination upon the ignition and burn process. Initial findings suggest that carbon impurities are quite tolerable. Further simulations are being carried out to extend the parameter space of the current study.

Acknowledgements

Simulations carried out for this study were carried out with the support of the STFC Rutherford Appleton Laboratory's Central Laser Facility's Plasma Physics Group. We are particularly grateful to Raoul Trines for maintaining the code at the CLF and to Peter Norreys the head of the Plasma Physics Group at the CLF.

The results shown in figure 2, from a previous study, were produced with the corporate support of General Atomics. We would like to thank Rich Stephens of General Atomics for contributions to this study, which is referenced below [4].

References

1. M. Tabak, J. H. Hammer, E. M. Campbell *et al*., Lawrence Livermore National Laboratory patent disclosure, IL8826B, (1997).
2. M. Tabak, J. Hammer, M. E. Glinsky, W. L. Kruer, S. C. Wilks, J. Woodworth, E. M. Campbell and M. D. Perry, *Phys. Plasmas*, **1**, 1626, (1994).
3. J. Nuckolls, L. Wood, A. Thiessen and G. Zimmerman, *Nature*, **239**, 139-142, (1972).
4. J. Pasley and R. Stephens, *Phys. Plasmas*, **14**, 054501, (2007).
5. HYADES is a commercial product of Cascade Applied Sciences, email larsen@casinc.com